

## Thermal Transitions and Barrier Properties of Olefinic Nanocomposites

David J. Chaiko\* and Argentina A. Leyva

Argonne National Laboratory, Chemical Engineering Division, 9700 South Cass Avenue,  
Argonne, Illinois 60439

Received April 1, 2003. Revised Manuscript Received October 1, 2004

Differential scanning calorimetry (DSC) was used to study the thermal transitions of smectite organoclays and their dispersions in olefinic systems, which included paraffinic waxes and polyethylene. The organoclays, with treatment on both the basal and edge surfaces, produced nanoscale dispersions without the aid of external coupling agents or compatibilizers. In addition to DSC measurements, the nanocomposites were further characterized using X-ray diffraction and oxygen transmission. The DSC measurements indicated that a clay/wax nanocomposite phase was generated with melt/freezing transition temperatures that were different from those of the individual components, while X-ray data indicated that the nanocomposite phase was in equilibrium with an intercalate phase. Barrier improvement of over 300× was observed and ascribed to a tortuosity effect resulting from dispersed clay platelets having a high aspect ratio and strong cohesion between the wax and the organoclay surface. Available data indicate that the barrier enhancement decreases as the difference between the freezing points of the organoclay and the wax widens. The cause of poor barrier performance in polyolefin systems is traced to the large difference in recrystallization temperatures, such that when the polymer begins to crystallize the surface of the organoclay is still in a liquid state, which leads to phase separation.

### Introduction

Since the late 1980s a great deal of research around the world has focused on developing methods to incorporate fully exfoliated smectite clays into polymers to increase mechanical and barrier properties.<sup>1</sup> The approach relies on organoclay technology developed by Jordan<sup>2</sup> in the 1950s, wherein the clay surface is treated to render it compatible with hydrophobic materials such as polyolefins and waxes. This surface treatment consists of an adsorbed monolayer of a high-molecular-weight quaternary amine, such as dimethyl dihydrogenated tallow amine. The surfactant adsorption takes place via an ion-exchange reaction involving the negatively charged basal surface of the clay platelets.

The simple mechanism by which the organoclays can improve barrier properties relies on the high aspect ratio of the exfoliated clay platelets to impart a tortuous path that retards the transport of diffusing species such as oxygen or water vapor. In a strictly tortuous path mechanism, all diffusing species would be retarded to the same degree. The tortuosity factor can be as high as several-hundred-fold for impermeable platelets with aspect ratios of 100–500 and at modest mineral loadings of 5–10 vol %.<sup>3</sup> Unfortunately,

nanocomposite performance has not always lived up to expectations, and barrier improvements of 2- to 4-fold or less are more typical.<sup>4</sup> It is becoming clear that the nature of the interphase surrounding the clay platelets, the basal surfaces as well as the clay edges, exerts a profound influence on gas permeation in nanocomposite systems.

To appreciate the challenges involved in producing olefinic nanocomposites exhibiting improved barrier properties, one must first consider the morphology of the polymer system. The polyolefins, together with the waxes, are semicrystalline materials that consist of a mixture of crystalline and amorphous phases at room temperature. If the hydrocarbon chains are long enough, they will fold in on themselves to form crystallites, which in turn stack upon themselves to form spherulites.<sup>5</sup> The crystallites are generally on the order of 10–20 nm, while the spherulites can be on the order of 50–100 μm or larger (Figure 1). The crystallites are held together by amorphous chain segments that contribute to the strength of the material. If the hydrocarbon chain length is shortened sufficiently, as in the case of the waxes, the amorphous chain segments become less able to bridge the gap between the crystallites, and the material becomes brittle. Gas diffusion

\* To whom correspondence should be addressed. E-mail: chaiko@cmt.anl.gov.

(1) Pinnavaia, T. J.; Beall, G. W., Eds. *Polymer-Clay Nanocomposites*; John Wiley & Sons: New York, 2000.

(2) Jordan, J. W.; Williams, F. J. *Kolloid Z.* **1954**, *137*, 40.

(3) Cussler, E. L.; Hughes, S. E.; Ward, W. J., III; Aris, R. *J. Membr. Sci.* **1988**, *38*, 161.

(4) Arimitsu, U.; Makoto, K.; Akone, O. U.S. Patent 6,121,361, Sept. 19, 2000.

(5) Billmeyer, F. W., Jr. *Textbook of Polymer Science*, 2nd ed.; Wiley-Interscience: New York, 1971, pp 141–165.

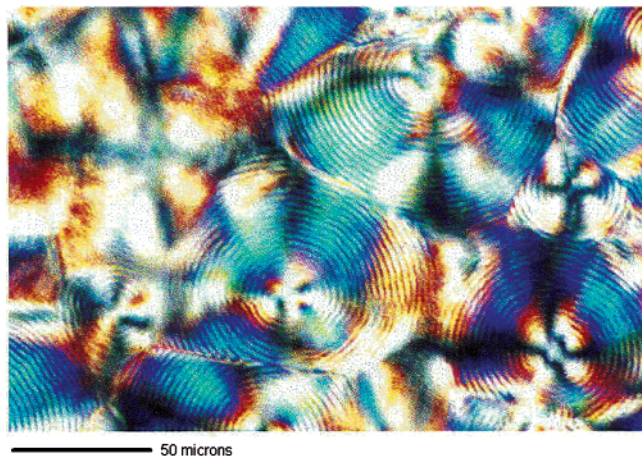


**Figure 1.** Ringed spherulites of high-density polyethylene visible under polarized light. The ring pattern results from the periodic twisting of the crystal lamella.

can take place at the interfaces between the crystallites and at the surfaces of the spherulites. Thus, a tortuous diffusion path is an inherent component of all semicrystalline wax and polymer systems.

Despite the chemical similarity between paraffin wax and low-density polyethylene (LDPE), they are not compatible because of the large difference in their freezing points — that is, their mixtures phase-separate upon cooling from the melt. By extension, we should not expect an organoclay that is prepared with paraffin-like surfactants to be compatible with either LDPE or the other polyolefins. One can envision the organoclay, along with any other impurities present in the polymer melt, being pushed aside and phase-separating from the crystallites during the polymer recrystallization process. Thus, it is not enough that the melted polymer wet the surface of the organoclay; the cohesion energy of the organoclay coating must be close to that of the wax or polyolefin crystal phase. In other words, the freezing points of the surfactant chains on the clay surface and the polyolefin must be close enough to enable the exfoliated organoclay to remain in solid solution as the nanocomposite phase freezes. We believe that this requirement will be true of all semicrystalline materials. Because of supercooling effects, recrystallization temperatures will be lower than the melting temperatures. In addition, the presence of the organoclay may affect the recrystallization temperature, especially if the organoclay is capable of acting as a nucleating agent. Therefore, the recrystallization temperature is expected to be a better predictor of solid-state miscibility than is the melting point.

In this article, we describe a new organoclay chemistry that enables the formation of paraffin wax nanocomposites demonstrating significant improvements in oxygen barrier properties. The improvements are on the order of 10–200× for low clay loadings and reach 10 000× at approximately 20 wt % loading. The barrier improvements can be described in terms of a tortuous path model. Differential scanning calorimetry was used to study the thermal transitions of the organoclay and their influence on nanocomposite formation and barrier performance in waxes and polyethylene. The data collected from these nanocomposite systems provide new

and interesting insights into the limitations of current organoclay designs, and help explain the poor barrier performance of current clay–polyolefin nanocomposites.

## Experimental Section

**Materials and Methods.** The organoclay used in this study was prepared from a Na<sup>+</sup>-montmorillonite (Cloisite Na, Southern Clay Products). The clay was dispersed in deionized water at a solids concentration of 2.5 wt %. The edge of the clay was rendered hydrophobic by reaction with the ammonium salt of 1-hydroxy-dodecane-1,1-diphosphonate (Solutia). The amount of diphosphonate added was 3 wt % relative to the weight of the dry clay. The temperature of the clay dispersion was then raised from room temperature to 70 °C, after which the basal surfaces of the clay platelets were modified by exchange with 110 meq of dimethyl dihydrogenated tallow ammonium chloride (Arquad 2HT-75, Akzo Nobel) per 100 g of clay. Combined with the quaternary amine were (a) poly(propylene glycol) with a molecular weight of 1000 at a concentration of 4 g per 100 g of clay, and (b) 2000 ppm Irganox B225 (Ciba) (contains 50% tris(2,4-di-(tert)-butylphenyl) phosphate and 50% tetrakis[methylene(3,5-di-(tert)-butyl-4-hydroxyhydrocinnamate)]methane) relative to the weight of the clay. The poly(propylene glycol) aids in the solvation of the organoclay surface by the wax by increasing the basal spacing of the organoclay. It functions in a manner similar to that of the low-molecular-weight polar activators used to aid dispersion of organoclays in mineral oils during the preparation of high-temperature greases.<sup>6</sup> The antioxidant (Irganox B225) is used to inhibit free radical damage during organoclay dispersion. After completion of the ion exchange reaction, the clay dispersion was filtered and then washed with deionized water. The organoclay was recovered as a pressed filter cake containing approximately 65 wt % water.

Wax nanocomposites were prepared by the slow addition of the organoclay to the melted paraffin wax (melting point of 50–55 °C, Aldrich) with stirring at 70 °C. The organoclay can be added as a filter cake or as a dried powder. When the filter cake is combined with the wax melt, the water is physically flushed from the surface of the clay to produce a separate water phase that can be mechanically separated from the wax melt. The advantages of filter cake flushing were recognized by Jordan<sup>2</sup> for its ability to minimize collapse of the organoclay platelets. Other nanocomposites were prepared with low-density polyethylene (LDPE) (Aldrich), and Parafliant H-1 (Moore & Munger), a high-temperature melting wax that is miscible with polyethylene. All of the polymer nanocomposites were prepared by flushing the water from the filter cake using the polymer melt in a twin-screw extruder (NFM Welding Engineers) that was modified to allow water removal as a liquid phase.<sup>7</sup>

The basal spacings of the nanocomposites were measured by X-ray diffraction with a Rigaku diffractometer with Cu K $\alpha$  radiation,  $\lambda = 1.541\text{\AA}$ . The oxygen transmission rate (OTR) was measured according to ASTM D 3985-9 on 50- $\mu\text{m}$  films that were applied to a silicone-release paper as a support. For polymer nanocomposite films, the OTR was measured from compression-molded films of approximately 125- $\mu\text{m}$  thickness. Differential scanning calorimetry (DSC) measurements were performed with a Perkin-Elmer Pyris 1 calorimeter under an argon atmosphere and at a scan rate of 10 °C/min.

## Results and Discussion

**Organoclay Chemistry.** Obtaining a nanoscale clay dispersion within a polymer matrix is not trivial. A complex

(6) Anonymous. *Rheology Handbook*; Rheox: Hightstown, NJ, 1998.

(7) Affeldt, D. C.; Pardi, M. F.; Teeley, C. M. U.S. Patent 6,348,091, Feb. 19, 2002.

balance of surface forces acting on the organoclay exerts a controlling influence that determines particle behavior. At high surfactant loadings, the geometry of the surfactant molecules on the organoclay surface possesses many of the attributes of a lamellar liquid crystal (LLC) phase<sup>8</sup>—close chain packing with a high tilt angle relative to the basal surface. Liquid crystals, by their very nature, are an intermediate state of matter being neither liquid nor solid. As such, organoclays will spontaneously swell in the presence of suitable organic solvents, but they will not spontaneously exfoliate and they tend to produce phase-separated systems—an organoclay intercalate in equilibrium with a pure organic phase. The inability of surfactant liquid crystals to solubilize significant amounts of oil has been studied by Friberg et al.<sup>9,10</sup> and this phenomenon is now known to be due to entropic effects, wherein the surfactant chains exhibit an order parameter that is intermediate between that of a liquid and that of a solid. Hence, the LLC phase is not compatible with a bulk isotropic liquid phase (e.g., a polymer melt).

The impact of surfactant order/disorder on organoclay dispersion was partially recognized in the mid 1950s by Jordan.<sup>2</sup> Specifically, it was shown that parallel alignment of the organoclay platelets, which could result from mechanical working of the wet filter cake prior to and during drying, markedly diminished the dispersability of the dried organoclay. An alternative to thermal drying was proposed by Jordan<sup>2</sup> that involved a solvent flushing technique to remove the water directly from the organoclay dispersion or the wet filter cake and thereby maintain the organoclay in a swollen state.

On the basis of what is known about surfactant liquid crystal systems, a useful approach to achieving a thermodynamically stable, exfoliated state would be to maximize entropic disorder within the surfactant coating (i.e., the quaternary amine monolayer). We have found that surface activation of the clay with low-molecular-weight polymers such as poly(ethylene glycol), poly(propylene glycol), and poly(tetrahydrofuran), coupled with treatment of the clay edge using the surfactant 1-hydroxydodecane-1,1-diphosphonate, promotes the stable dispersion of the organoclay in aliphatic solvents, waxes, and LDPE.<sup>11</sup> This behavior is in contrast to that of Cloisite 15A (i.e., Cloisite Na treated with 125 meq of dimethyl dihydrogenated tallow amine), which produced a brown precipitate when combined with the paraffin melt. Additionally, dispersions of Cloisite 15A in LDPE were opaque and white due to light scattering from agglomerated clay particles.<sup>11</sup> In contrast to this behavior, our organoclay produced a dark-green nanocomposite capable of remaining dispersed in the wax melt indefinitely. The green color results from the underlying color of the clay

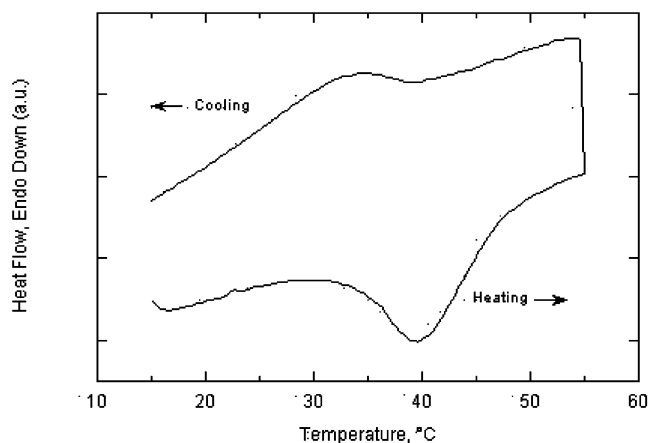


**Figure 2.** DSC curve for the organoclay containing 110 meq of dimethyl dihydrogenated tallow amine, poly(propylene glycol), and 1-hydroxydodecane-1,1-diphosphonate. The peak transition from the crystal phase to the LLC phase occurs at 39.6 °C while the recrystallization transition occurs at 34.4 °C with a  $\Delta H$  of  $-4.4$  J/g.

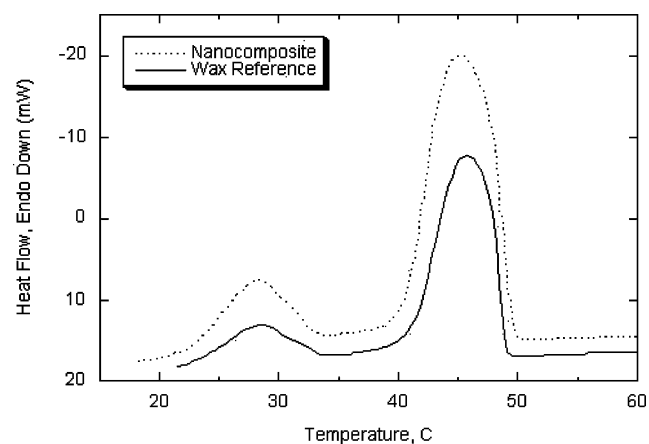


**Figure 3.** Cooling curve for paraffin reference and nanocomposite containing 10 wt % organoclay. The peak freeze transitions occur at occur at 45 and 28 °C. The combined heat of crystallization from both peaks for the wax and nanocomposite is 1.04 and 1.63 J, respectively.

crystal lattice, and we interpret its presence as an indication that the surface of the organoclay is being extensively solvated by the paraffin. We should also point out that polyethylene nanocomposites were similarly colored, but only when dispersed by flushing the organoclay filter cake with the polymer or with prolonged mixing of the dried organoclay (e.g., >30 min in a Brabender Plasticorder). This dependency on dispersion method was not observed with paraffin wax, and suggests that the initial polymer intercalation represents the rate-controlling step in clay exfoliation.

**Thermal Transitions.** In Figure 2 we show a DSC curve for our organoclay illustrating the melt/freeze transitions of the surfactant monolayer. There is a melting point associated with the crystal to LLC transition centered at 39.6 °C. During this transition, the alkyl chains melt to produce a liquid crystal phase. As the organoclay is cooled, there is a slight degree of supercooling before the liquid crystal phase freezes at 34.4 °C.

The cooling curves for the paraffin wax and the nanocomposite containing 10 wt % organoclay are shown in Figure 3. Two crystallization peaks were observed in both samples. The peak recrystallization temperatures for the wax occurred at 45.7 and 28.4 °C with  $\Delta H$  values of  $-136.8$  J/g

- (8) Collings, P. J.; Hird, M. *Introduction to Liquid Crystals*; Taylor & Francis: Philadelphia, PA, 1998.
- (9) Ward, A. J. I.; Friberg, S. E.; Larsen, D. W. In *Macro- and Microemulsions: Theory and Applications*; Shah, D. O., Ed.; ACS Symposium Series 272; American Chemical Society: Washington, DC, 1985; p 185.
- (10) Moucharrafieh, M.; Friberg, S. E.; Larsen, D. W. *Mol. Cryst. Liq. Cryst.* **1979**, 53, 189.
- (11) Chaiko, D. J. In *Affordable Materials Technology – Platform to Global Value and Performance*; Rasmussen, B. M., Pilato, L. A., Klinger, H. S., Eds.; SAMPE: Covina, CA, 2002; p 1064.



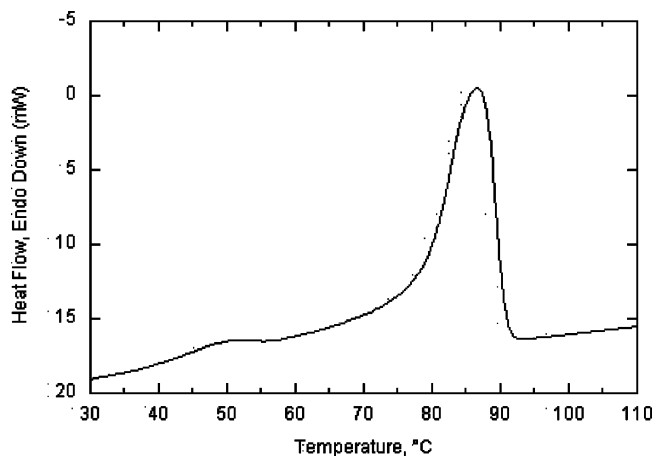


**Figure 4.** DSC cooling curve for 10 wt % organoclay + 90 wt % LDPE. Peak recrystallization temperatures for the polymer and organoclay are 86.6 °C and 50.3 °C, respectively.

and  $-26.6$  J/g, respectively. The peak recrystallization temperatures for the nanocomposite were 45.2 and 28.1 °C with  $\Delta H$  values of  $-127.0$  and  $-27.5$  J/g, respectively. The low-temperature transitions occur at temperatures similar to the LCC recrystallization transition observed in Figure 2, but the  $\Delta H$  values are significantly different (the value of  $\Delta H$  for the pure organoclay is only  $-4.4$  J/g). An obvious question to ask is whether the organoclay has any effect on the degree of crystallization. From a measurement of normalized peak areas, we find the total heat of crystallization for the paraffin is  $-0.99$  J, while for the nanocomposite the value is  $-1.66$  J. The degree of crystallization in the nanocomposite is higher than that in the reference. From this we may conclude that the organoclay acts as a nucleating agent.

The loss of the individual phase transitions (i.e., organoclay freezes at 34.4 °C) and the appearance of only one set of melt transitions and one freeze transition in this two-component system suggests that the organoclay/wax nanocomposite consists of only a single phase. However, as we will show later, X-ray data indicate that the nanocomposite does contain some unexfoliated organoclay; hence it is, in fact, a two-phase system in which the organoclay is in equilibrium with the nanocomposite phase. Characteristic of LLC phases in general, the organoclay phase transitions are low-energy transitions.<sup>8</sup> It is likely that the organoclay transitions are present in the nanocomposite but that they are simply too weak to be detected by the calorimeter. On the other hand, the DSC data indicate that the exfoliated clay + paraffin (i.e., the nanocomposite phase) is indeed a new phase and not just a physical mixture of exfoliated clay and wax.

As we will show later, the appearance of a nanocomposite phase has a profound impact on barrier properties. In contrast to the paraffin system, the DSC curve for the organoclay/LDPE system in Figure 4 clearly shows separate freeze transitions for the clay and polymer. Interestingly, the organoclay freeze transition increased from 34.4 to 50.6 °C in the presence of the polymer, suggesting that there is some interaction between the two. However, we can still expect the large difference in recrystallization temperatures to lead to the formation of two separate organoclay and polymer

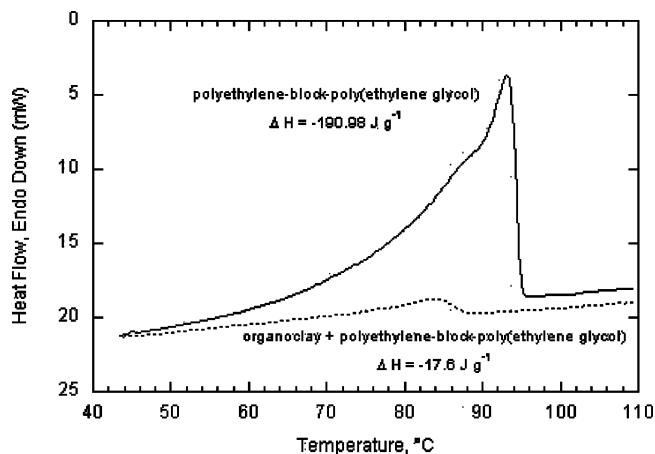


**Figure 5.** Cooling curves for polyethylene-*block*-poly(ethylene glycol) and the nanocomposite containing 70 wt % organoclay/30 wt % polyethylene-*block*-poly(ethylene glycol). Approximately equal sample weights were used in the DSC measurements. Peak freezing points are 91.3 °C for the copolymer and 83.5 °C for the nanocomposite.

phases when the melt is cooled to below the recrystallization temperature. The barrier properties of this material will be discussed later.

**Limitations of Current Organoclays.** To overcome the difficulties in exfoliating organoclays in hydrophobic polymers such as the polyolefins, researchers have used functionalized polymers, such as maleated polyethylene and polypropylene, as dispersants.<sup>12</sup> While polar functional groups can interact with the organoclay surface and compatibilizing agents can promote exfoliation, the presence of organoclay thermal transitions would still be present and, if not matched to the polymer, would create a highly permeable interphase surrounding the organoclay. While this approach to nanocomposite formation has been shown to provide modest improvements in the mechanical properties of polyolefins,<sup>13</sup> we are not aware of any published results that show increased barrier toward oxygen or water vapor in polyolefins or waxes.

Our use of poly(propylene glycol) is an attempt to introduce disorder within the quaternary amine monolayer. Another approach we have taken is the use of cosurfactants such as *n*-alkyl poly(ethylene glycol). The latter approach is based on the fact that the lamellar phase of *n*-dodecyl tetraethylene glycol ether is reported<sup>9</sup> to be capable of solubilizing hydrocarbons to such an extent that an isotropic liquid hydrocarbon layer forms between the layers of surfactant molecules. We have found that incorporating polyethylene-*block*-poly(ethylene glycol) as a cosurfactant with the quaternary amine leads to improved dispersability in polyolefin systems.<sup>11</sup> Attachment of this unusual surfactant, which contains a 50-carbon alkyl chain, enables us to raise the effective melt and recrystallization temperatures of the organoclay surface.

The DSC data in Figure 5 are the cooling curves for the polyethylene-*block*-poly(ethylene glycol) and the clay/

(12) Okada, A.; Fukushima, Y.; Kawasumi, M.; Inagaki, S.; Usuki, A.; Sugiyama, S.; Kurauchi, T.; Kamigaito, O. U.S. Patent 4,739,007, April 19, 1988.

(13) Gopakumar, T. G.; Lee, J. A.; Knotopoulou, M.; Parent, J. S. *Polymer* **2002**, *43*, 5483.

**Table 1. Oxygen Permeability of Clay/Wax Nanocomposite Films**

organoclay (wt%)	permeability (mol O <sub>2</sub> /m <sup>2</sup> ·s·Pa)
paraffin reference	4629 × 10 <sup>-17</sup>
5	75 × 10 <sup>-17</sup>
10	14 × 10 <sup>-17</sup>
15	4629 × 10 <sup>-17</sup>
Parafint H-1 reference	3404 × 10 <sup>-17</sup>
10	2393 × 10 <sup>-17</sup>

polymer nanocomposite containing 70 wt % organoclay. The presence of the organoclay reduced the peak freeze temperature of the polymer from 92.6 to 84 °C, suggesting the presence of a nanocomposite phase having thermal transitions that are intermediate to those of the individual components. However, the freeze transition at about 40 °C present in the pure organoclay was still detectable in the nanocomposite. The X-ray diffraction pattern of the nanocomposite indicated that the clay was exfoliated despite the high clay concentration.<sup>11</sup> While coupling agents or compatibilizing agents (e.g., maleated polyolefins) may help disperse the organoclay and aid in the formation of nanocomposites, the fact remains that the phase transitions of the quaternary amine are likely to still be present, and can be expected to lead to grain boundary defects that would provide an unimpeded path for gas transport.

**Oxygen Permeability.** Wax nanocomposites, at various organoclay concentrations, were prepared and applied as a thin coating to the surface of a silicone release paper. The oxygen transmission rate (OTR) was measured using cast films with a thickness of approximately 50 μm. The measured film thickness (*L*) was used to calculate oxygen permeability (*P*) from the OTR data (i.e.,  $P = \text{OTR} \cdot L$ ). The results for three different organoclay loadings in paraffin wax are reported in Table 1 along with the reference value for the clay-free system. There is a dramatic decrease in oxygen permeability with increasing organoclay concentration except for the highest loading at 15 wt %. With only 5 wt % organoclay, the oxygen permeability dropped by approximately 62×. Increasing the clay loading to 10 wt % reduced the oxygen permeability by a factor of 330× relative to the clay-free system. However, continued increase in the organoclay concentration led to embrittlement of the film that was accompanied by a complete loss of any barrier improvement. Microscopic examination of the film with 15 wt % organoclay revealed extensive cracking with the result that the nanocomposite film looked identical to the reference film. A control experiment in which 5 wt % Cloisite 15A was dispersed in the wax showed no measurable change in oxygen permeability relative to that of the pure wax.

If we assume that the decrease in gas transport is due to a tortuosity effect derived from an inert filler, we can use the measured permeability data to calculate the effective aspect ratio of the organoclay platelets. To judge how well the tortuosity model fits the data, we can compare the calculated aspect ratios with known values for smectite clays such as Cloisite Na. A tortuosity model for mineral-filled polymer systems has been described in the literature.<sup>3</sup> The model relates the permeability ratio ( $P_o/P_f$ ) to the aspect ratio ( $\alpha$ ) of the filler and the filler loading ( $\phi$ ). If the gas permeability is limited by diffusion through narrow gaps

**Table 2. Peak Melt/Recrystallization Temperatures for Various Waxes and Polymers**

system	peak melt temp, °C	peak freeze temp, °C
organoclay	39.6	34.4
paraffin wax	56.2	45.5
10 wt % organoclay/90 wt % paraffin	52.4	44.7
Parafint H-1	100.6	87.0
LDPE	102.9	87.4

between the oriented clay platelets, the relative permeability is given by

$$P_o/P_f = 1 + \frac{1}{2} \alpha \cdot \phi \quad (1)$$

where  $P_f$  is the permeability of the mineral-filled composite and  $P_o$  is the permeability of the unfilled system. On the other hand, if the permeability is limited by gas diffusion around impermeable clay platelets, the relative permeability becomes proportional to the square of both the aspect ratio and the clay loading

$$P_o/P_f = 1 + \frac{\alpha^2 \cdot \phi^2}{(1 - \phi)} \quad (2)$$

When we used eq 1 to calculate the aspect ratio of the organoclay platelets in our wax nanocomposites at 5 and 10 wt % loading we obtained values of approximately 3 000 and 9 500, respectively. These values are well beyond the expected aspect ratios for montmorillonite, which are reported to be between 100 and 500.<sup>1</sup> When we used eq 2 to calculate the effective aspect ratio, we obtained values of 250 and 240 at 5 and 10 wt % loading, respectively. These values are well within the expected range and, as we might expect, are independent of clay loading. Clearly, the mechanism by which the oxygen permeability is reduced is by a tortuous path in which the permeability is limited by diffusion along the surface of the clay platelets.

Table 1 also contains oxygen permeability data for a nanocomposite made with a Parafint H-1, which has a freezing temperature equal to that of LDPE. In this case oxygen permeability was reduced only 30% relative to the pure wax. This is in contrast to the paraffin wax nanocomposite, which demonstrated a 98.4% reduction in oxygen permeability at similar clay loading. We believe these data support the hypothesis that freezing point of the organoclay and the polymer phase must be sufficiently close to each other to ensure solid-state miscibility of the clay within the nanocomposite. The peak melt and recrystallization transitions for several wax and polymer systems are listed in Table 2. As we have shown, miscibility of two or more components requires a close match between the individual recrystallization temperatures. For example, Parafint H-1 and LDPE have peak recrystallization temperatures that differ by only 0.4 °C, and these materials are miscible in both the melt and solid states.

While maintaining the clay in an exfoliated state is important, it may not be the only determining factor affecting barrier performance. We believe the inability of an isotropic polymer phase to wet and bond with an anisotropic organoclay surface is also a contributing factor responsible for

**Table 3. Relationship between Oxygen Barrier, Polymer Molecular Weight, and Recrystallization Temperature**

system <sup>a</sup>	Olefin MW	peak freezing temp, °C	% reduction in O <sub>2</sub> permeability
paraffin	~400	45.5	98.4
Parafint H-1	785	87	36.9
LDPE	>40,000	86.6	0

<sup>a</sup> Nanocomposite systems all contain 5 wt % organoclay.

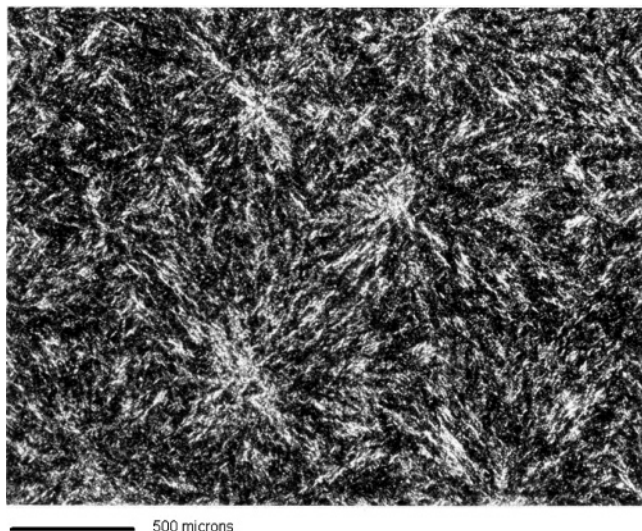


**Figure 6.** Polarized light micrograph of a clay/wax nanocomposite containing 5 wt % organoclay.

the poor barrier performance observed in polyolefin systems. In other words, while it may be relatively easy for a paraffin molecule to suffer the loss in entropy necessary to adopt a favorable orientation to interact with the LLC phase, it is unlikely that the significantly greater loss in entropy accompanying the uncoiling of a high-molecular-weight polymer could be compensated sufficiently by changes in enthalpy. This hypothesis is supported by the data in Table 3, which show the effects of freezing points and molecular weight on oxygen barrier. As the olefin chain length is increased from paraffin to LDPE, we see a steady decline in the influence of the organoclay on oxygen transmission. This can be partially explained by the fact that an increase in chain length is accompanied by an increase in recrystallization temperature, which would lead to phase separation of the clay during cooling of the polymer melt. However, while the recrystallization temperatures of Parafint H-1 and LDPE are virtually identical, the wax nanocomposite still exhibits some improvement in barrier properties while the LDPE system shows no change in OTR.

**Effect of Clay on Wax Crystallization.** To better understand how the organoclay might affect the solid-state morphology of the wax, we examined the microstructure of the nanocomposites using polarized light microscopy. The photomicrograph of the wax nanocomposite in Figure 6 shows that the organoclay has a dramatic influence on the crystal structure of the wax. Normally, a significant amount of shrinkage accompanies wax recrystallization due to the high degree of crystallinity and the large density difference between the amorphous melt and the crystal phase. This shrinkage leads to extensive cracking. However, the nanocomposite with 5 wt % organoclay did not exhibit the

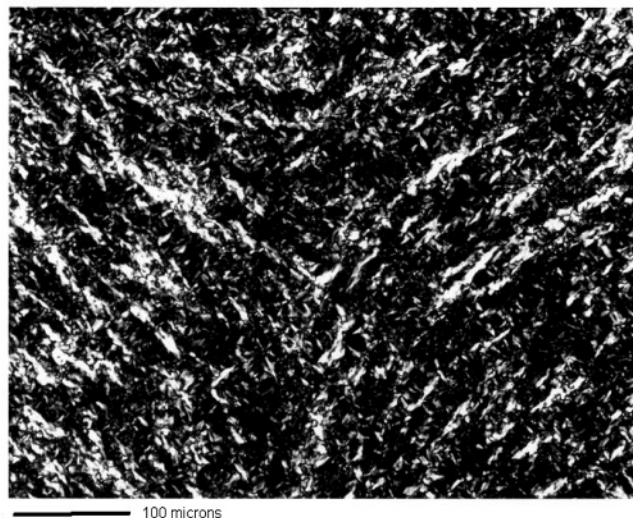


**Figure 7.** Crystal structure detail at the spherulite interface of a clay/wax nanocomposite with 5 wt % organoclay.

shrinkage that normally occurs in paraffin wax. The higher magnification of Figure 7 shows that a distinct boundary between wax spherulites is noticeably absent, and in fact the crystallites appear to bridge the gap between adjacent spherulites. In other words, the organoclay appears to have reduced the shrinkage that would normally occur at the boundaries of the wax spherulites. The result is a much more densely packed film with fewer structural defects. However, adding too much clay leads to embrittlement and cracking of the cast films. Microscopic examination of the nanocomposite with 15 wt % organoclay showed a complete loss of the spherulite structure. It appears that sufficiently high organoclay concentrations can inhibit the normal bonding that occurs between wax crystallites and at the spherulite surfaces.

We attempted to plasticize the wax nanocomposite with polyethylene to reduce the embrittlement at high clay loading. We first combined the organoclay with an approximately equal weight of polyethylene-*block*-poly(ethylene glycol) by melt compounding at 130 °C. We should point out that in this case the organoclay was prepared without the poly(propylene glycol) additive, as it might have blocked the surface adsorption sites that are required to anchor the copolymer. The organoclay/copolymer mixture was then compounded with a 50:50 blend of paraffin and LDPE. The final organoclay concentration in the nanocomposite was 21.8 wt %, as calculated from ash analysis. Despite the high clay loading, the cast nanocomposite films were quite flexible and free of gross structural defects. The photomicrograph in Figure 8 shows that the presence of the clay in the LDPE hybrid has completely inhibited spherulite growth. The measured oxygen permeability of the film was  $0.5 \times 10^{-17}$  mol/m<sup>2</sup>·s·Pa. This represents a 9000× reduction in permeability relative to the wax reference and some 300× lower than the LDPE reference. To put this in perspective, the remarkably low permeability of this nanocomposite hybrid is equal to published values for nylon-6, which is considered to be a high-barrier polymer.<sup>14</sup>

(14) Combellick, W. A. In *Encyclopedia of Polymer Science and Engineering*, Vol. 2; John Wiley & Sons: New York, 1985; p 180.



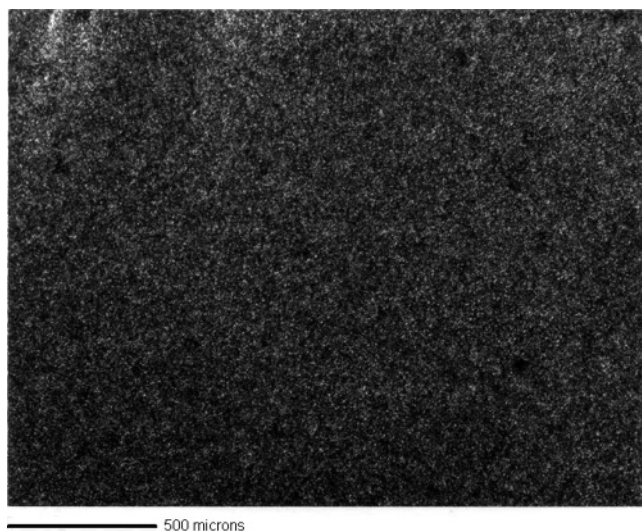


**Figure 8.** Polarized micrograph of a clay/wax/polyethylene nanocomposite containing 21.8 wt % organoclay.

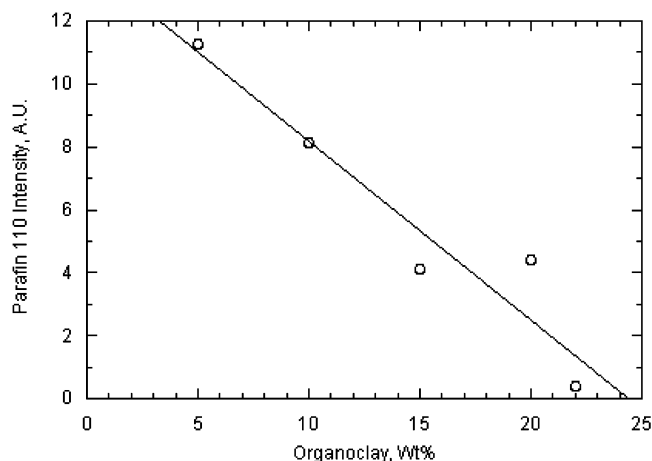


**Figure 9.** Plot of paraffin  $d_{110}$  diffraction peak intensity as a function of organoclay loading.

To further understand the mechanism responsible for the unexpectedly high barrier properties of the wax-containing nanocomposites, we measured the relative wax crystallinity as a function of organoclay loading. The normal 3-D crystal phases of both paraffin and LDPE exhibit an X-ray diffraction peak at approximately  $4.1 \text{ \AA}$ , which corresponds to the  $d_{110}$  spacing. We have found a direct correlation between the height of this diffraction peak and organoclay loading. This interesting result is shown in Figure 9.

We have assumed that the height of the  $d_{110}$  diffraction peaks is proportional to the mass ratio of crystal/amorphous

phases in the wax. Because the melt history, the diffraction geometry, and the aging of the samples remained constant, we believe these assumptions are reasonable. The data in Figure 9 suggest that the exfoliated organoclay inhibits the formation of the 3-D wax crystal. For this to occur, the cohesion energies of the wax and organoclay crystal phases must be approximately equal (by organoclay crystal phase we are referring to the alkyl chains of the quaternary amine). If normal crystal formation is inhibited, we may expect a confined, 2-D wax crystal phase to grow between adjacent organoclay platelets. Interestingly, similar conclusions regarding crystal growth were reported recently in a study of high-density polyethylene nanocomposites.<sup>13</sup>

## Conclusions

Using organoclays with modifications to both the basal and edge surfaces, we were able to prepare paraffinic wax nanocomposites demonstrating improved oxygen barrier performance. A series of nanocomposites was prepared with increasing molecular weight, ranging from paraffin wax to LDPE. The materials were characterized by DSC, OTR, and X-ray diffraction measurements. Improved gas barrier capability can be ascribed to the appearance of a new nanocomposite phase demonstrating a single set of melt/freeze transitions. Increasing the molecular weight of the wax led to a decrease in barrier performance. This behavior is ascribed to the fact that while an organoclay may produce a homogeneous nanocomposite phase in the melt state, phase separation and grain boundary defects can occur when the wax recrystallizes if the surface of the organoclay is still in a liquid state when this occurs. The failure to produce improved barrier performance in polyolefins appears to be the result of a combination of factors, which include thermal transition effects and the inability of an isotropic polymer phase to wet and bond with an anisotropic organoclay surface. The use of coupling agents such as maleated-polyethylene or maleated-polypropylene would not affect the thermal transitions of the quaternary amine and should not be expected to lead to improved barrier capabilities.

**Acknowledgment.** This work was supported by the U.S. Department of Energy, Office of Nuclear Energy, Science and Technology, under Contract W-31-109-Eng-38. We thank Dr. Tim Hirzel of Solutia for synthesizing the alkyl diphosphonate.

CM0302680